EXPERIMENTAL COMPARATIVE STUDY OF THE APPLICABILITY OF INFRARED TECHNIQUES FOR NON-DESTRUCTIVE EVALUATION OF PAINTINGS

DMITRY GAVRILOV[1], ELENA MAEVA[1], OLEG GRUBE[2], IGOR VODYANOY[3], AND ROMAN MAEV[1]

[1] *Institute for Diagnostic Imaging Research, University of Windsor, Canada*
[2] *Tessonics Corp., Canada*
[3] *Office of Naval Research, USA*

Noninvasive methods of near-infrared, short-wave infrared, and thermographic inspection of artwork are described in this article and compared in terms of their ability to reveal both hidden graphite underdrawings and subsurface degradations. This inspection aids the understanding of the artist's work methods and locates hidden areas of damage. While all three inspection methods are suitable for locating sketches and changes in composition, this study has proven that thermographic methods are very useful in detecting structural defects such as delaminations and cavities, as demonstrated with experiments conducted on test samples and real paintings.

KEYWORDS: *thermography, nondestructive, analysis, defectoscopy*

1. INTRODUCTION

Structural analysis of objects of art is often performed by collecting images of the artwork under study in various spectral bands. Due to the higher penetrability of longer wavelengths into material, the infrared band is of particular interest and is widely used by museums and restoration laboratories. Depending on the particular spectral range used, near-infrared imaging (NIR, 0.7–1.1 μm) and short-wave infrared imaging (SWIR, 1.1–2.5 μm) methods can be distinguished. Longer wavelengths bands, namely middle-wave infrared (MWIR, 3–5 μm) and long-wave infrared (LWIR, 8–14 μm), are used by thermographic analysis methods and are more common for industrial analysis.

This work addresses the thermographic inspection technique once again and compares the results it provides with those of NIR/SWIR imaging of specifically designed oil paintings such as layered icon-like samples and oil paintings on canvas to demonstrate that thermographic inspection can be as useful as NIR/SWIR while providing information that neither NIR nor SWIR can produce.

2. THEORY

2.1 NIR AND SWIR REFLECTOGRAPHY

NIR and SWIR techniques that are primarily photographic in nature were proven to be good tools for finding altered areas as well as artists' sketches sometimes present at the ground layer. Lyon (1934), King (1936), Farnsworth (1938), Desneux (1958), Heiber (1968), Van Asperen de Boer (1968), and others demonstrated successful case studies that revealed *pentimenti*, touch-ups, and other artifacts. Using the Kubelka-Munk theory (Van Asperen de Boer 1968, 1969) it was demonstrated that many of the pigments used in art are nearly transparent while the observation is conducted within NIR/SWIR wavelengths. The peak of transparency was shown to be reached near 2.0 μm, which has also been addressed recently by Gargano et al. (2007).

Thus, using wavelengths longer than those of the visible band allows for visualization of those materials that are located underneath optically opaque art materials. In particular, such materials as charcoal and graphite often used for sketches may be located due to the high opacity of carbon in the infrared band up to about 4 μm (Friedel and Hofer 1970, 1971).

Although SWIR-detecting devices usually provide better results than those working in NIR due to the peak of transparency of pigments around 2.0 μm, SWIR devices are often much more expensive than NIR-detecting tools. For that reason, many museums and laboratories often use specially modified conventional digital photographic cameras with silicon charge-coupled device (CCD) or complementary metal oxide semiconductor light detectors. The modification

© American Institute for Conservation of Historic and Artistic Works 2013
DOI: 10.1179/019713601 2Z.0000000002

involves removing the visible-pass filter put in by the manufacturer. Such detectors can detect the visible band and up to about 1.1 μm (Falco 2009); this limit is determined by the value of the energy gap in silicon (1.1 eV at room temperature) (Moss 1959; Wright 1966). A digital camera modified that way may be set up for NIR photography by using an infrared-pass filter, e.g., Wratten 88A, Wratten 87, Wratten 87C (in this work Wratten 87 from PECA Products Inc. was utilized) or similar. Among the main advantages of such devices over SWIR detectors are low cost and high resolution, which is why CCD devices are widely used for art analysis purposes.

2.2 THERMOGRAPHY

Another type of nondestructive testing utilizes MWIR and LWIR. All moderately heated objects emit radiation in these bands. The investigative method used to analyze objects through external temperature stimulation is *thermography*. This technique, though relatively new to art analysis in comparison with NIR/SWIR imaging, has shown very promising results in the analysis of painted panels (Miller 1977; Ambrosini et al. 2010), frescoes (Grinzato et al. 1994; Bendada et al. 2010), mosaics (Avdelidis et al. 2007), etc., for the presence of mechanical defects such as cracks, delaminations, and moisture. Also, thermography is actively used for historical buildings inspections (Avdelidis and Moropoulou 2004; Meola et al. 2005; Grinzato et al. 2010).

Thermographic examination is based on the study of the temperature signature of the sample of interest. In contrast to *passive thermography*, which is a study of heat-generating objects, *active thermography* utilizes a source of external heat which provides temperature excitation to the sample, which initiates heat fluxes. These fluxes may result in different temperature patterns on the surface of the sample depending on the internal structure of the sample tested (Maldague 2001). Thus, the information about the internal part of the sample can be extracted from a surface temperature distribution, which can be determined with a thermal imager and processed with a computer. Since most of pieces of art do not generate heat themselves, the active approach is of main interest in noninvasive inspection of artworks.

The heat energy pulse can be applied to the sample using many readily available sources such as a flash lamp for example. The surface temperature of the sample will be changing with a time rate correlating to the heat-conducting properties of the sample. In case of partial area delamination or crack, the surface temperature decay will be slower in that region, thus revealing otherwise hidden defects of the sample structure. After the stimulation, the surface temperature evolution is recorded by means of a thermal camera in the form of a series of snapshots taken with a certain frame rate and stored by a computer. The outcome of this process is a three-dimensional array of data on the temperature evolution for all points in the field of view of the thermal camera. Such a 3D array is sometimes referred to as a *thermogram* and can be either used for finding the frame best uncovering internal defects or for further processing in order to increase the quality of the data (e.g. noise suppression).

The approach with no or minor processing of raw thermograms, known as pulsed thermography, is a fast, and in many cases reliable, technique allowing for an express defectoscopy (Maldague 2001). However, the thermal variations produced on the surface by deep and/or small-sized artifacts can be smaller than thermal variations caused by nonuniformity of surface heating. On the other hand, the nonuniformities themselves can be misinterpreted as subsurface voids (Miller 1977). Thus, for a successful detection of subsurface artifacts a technique capable of correcting heating nonuniformity as well as highlighting small changes in temperature must be employed.

There are a number of techniques available for correcting the effect of nonuniform heating, denoising, and enhancement of thin artifacts detectability. Among them, pulse phase thermography (PPT) has been successfully applied to the analysis of canvas-based paintings (Gavrilov et al. 2008). The main principle of PPT is representation of the raw data as a series of decaying harmonic signals, which have various depths of penetration in the bulk of material (Maldague 2001). Constructing images containing the phase of these harmonic signals allows for significant noise reduction as well as depth information extraction if the thermal properties (thermal diffusivity) of the material are known. Another approach, known as Thermal Signal reconstruction (Blessley et al. 2010), works on the premise that the surface temperature of the nondefective area of the sample decays proportionally to inverse square root of time and any deviation from this trend would indicate the presence of a subsurface feature. Determining the presence of such deviations allows for locating the defective areas and finding the time moment when this deviation occurs – the depth information can then be determined, provided the thermal properties of the material are known. The common point of these two methods is that they utilize a particular form of solution of the heat equation – either damped harmonic or exponential decay solution.

The method used in this work is based on the principal component thermography (PCT) method introduced by Rajic (2002) based on a data-processing method known as principal component analysis (PCA) discussed in a number of works (Daultrey 1976; Jolliffe 2002). PCT is not based on a particular

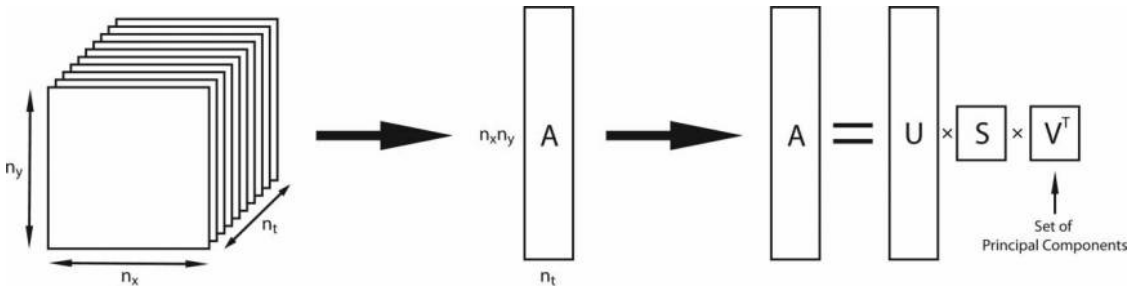

FIG. 1. An explanation of PCT data processing. The 3D array of raw thermographic data is first converted into a 2D array, which is then converted into a product of three matrices. Matrix V contains a set of principal components, representing the "temperature trends."

physical model; it is rather a statistical processing of the raw thermographic data and requires no information on the thermal properties of the sample studied. This may be convenient for an analysis of objects of art where the exact properties of the materials used are unknown.

The core of the method is the representation of the raw thermographic data array as a set of vectors – 1D sets of numbers corresponding to temperatures of a particular point of the surface at different moments in time. If plotted as a graph, each of these vectors would demonstrate how the temperature of a particular point of sample was cooling down after the initial stimulation. Then, with the aid of the singular value decomposition procedure all vectors are processed to extract a set of new vectors of the same size representing "temperature trends" in the initial vector set (fig. 1). This operation is reversible, so the initial set of vectors can be reconstructed using the temperature trends found.

The first of the new vectors (called the first principal component) represents the main shape of the temperature decay, which is the most common trend of the initial set of data, the second vector (the second principal component) represents variations that are less common for the entire set of data (variations from the common trend), and so on. The last vectors in the new set of vectors represent temperature variations, which are specific for individual points of the sample surface. Most often the last principal components correspond to detector noises (Hermosilla-Lara et al. 2002; Vavilov et al. 2008).

Assuming that the temperature changes differently in defective and nondefective areas of the sample, one would be interested in highlighting this difference in order to recognize the presence of a defect or a subsurface feature. For this reason, it is promising to reject the contribution of the first couple of vectors (thus, removing the most common features of the temperature decay) and the last vectors (noise) by manually reducing the size of matrices U, S, and V, and then recombine the initial data set back (fig. 1). This reconstructed data set reflects minute differences between temperature behaviors of areas of the sample and can be used for finding the final image illustrating the defects or subsurface features present. It is important to note that the rejection of one or more principal components forbids treating the final image as a thermal image.

3. Instrumentation And Experimental Setups

For NIR testing, the forensics-designed Fujifilm Finepix S3 Pro UVIR camera equipped with a silicon CCD detector having NIR wavelength sensitivity of up to 1100 nm was the instrument of choice for conducting the analysis. The Wratten 87 NIR-pass filter was used to block the visible band so that the range of the wavelengths used was 750–1100 nm.

SWIR inspection was carried out with a XenICs Xeva 1.7-320 camera. This camera is equipped with 320 × 256 indium–gallium–arsenide (InGaAs) detector sensitive to 0.9–1.7 μm and is connected to a computer via a USB interface.

NIR and SWIR inspection were carried out in a reflection scheme, where the NIR-sensitive camera and the source of light are located on the same side of the sample. An incandescent 150 W light bulb was used as a source of illumination.

The thermal imager FLIR SC4000 (sensitive to wavelengths of 3–5 μm) aided in the thermal experiments. The device has a 320 × 256 indium–antimonide (InSb) detector and a flexible frame rate (100–400 fps was achievable with the available computer configuration). The connection to a computer was established with gigabit Ethernet (GigE) interface.

The samples in this study were thermally excited by a short heat pulse application. For creating a short pulse, a Speedotron 4803CX system with a single Speedotron 206VF light unit was used. The light bulb used was MW40QC with color temperature $T_c = 5500$ K (nearly as bright as noon daylight).

The flash duration was set to 1/175 seconds and the maximum temperature of the sample during the flash was within the range of 30–40°C. The flash unit was arranged in a position allowing for oblique (45° was the angle of choice) light illumination of the object and

excluding possible direct light reflection from the flash into the imaging device. The thermographic experiments were conducted using a reflection scheme.

Acquired thermograms were processed with MATLAB software, for which an algorithm able to perform PCA and manipulate certain principal components as described in the theory section was developed. After the thermograms were collected, the software was set to neglect the first component. In cases where it was necessary, the second principal component was neglected as well in order to enhance the visibility of subsurface feature(s). In order to suppress detector noise principal components with orders higher than 20 were also neglected.

During all experiments (NIR, SWIR, and thermographic), partial images were acquired from different parts of samples and the final images were stitched together afterwards using graphic editing software (Adobe Photoshop CS5).

The samples tested included:

1. A piece of pre-gessoed canvas with 25 4 × 4 cm regions with lead pencil drawings. The regions were covered with various oil paint pigments (fig. 2) from a range of manufacturers.
2. A simulated 15.2 × 13.8 cm panel painting (fig. 3). A poplar panel was selectively covered with animal glue before the application of gesso and prior to making the painting. Due to the lack of adhesion between gesso and the support in the region with no glue, a delamination has formed (Gavrilov et al. 2010).
3. Two oil canvas-based paintings: unattributed painting depicting a portrait of a young woman (fig. 4) and "Portrait of an old musician with flute" by Thomas Faed (fig. 5). The sizes of the paintings are as follows: 49.5 × 41.8 cm for the portrait of the young woman, and 35.8 × 25.5 cm for the "Musician" (Gavrilov et al. 2010). Both samples are owned by a private collector in Windsor, Canada.
4. An icon (fig. 6). Tempera on wood. 28 × 20.5 cm (Gavrilov et al. 2010). The piece is owned by a private collector in Windsor, Canada.

For the purpose of analysis the images of all samples were taken in visible light spectral band, NIR band, and SWIR band. Thermographic analysis included the application of a short (~1/175 seconds) flash pulse, collection of images in MWIR spectral band, and subsequent enhancing of the images by the application of PCA.

4. Results

4.1 The canvas patches with pigments

Due to the transparency of certain paints, the presence of lead pencil sketches is well-observable on 3 of 25 patches with the unaided eye (fig. 2). These are the squares corresponding to cadmium red, madder lake deep, and madder lake light.

When the sample is observed in near-infrared band, the sketches are barely detectable in the entire top row (naples yellow, naples yellow light, naples yellow red, and French ultramarine). The graphite sketches can be clearly seen under such pigments as cobalt blue, cerulean blue, ultramarine deep. The sketches covered with cadmium red, madder lake deep, madder lake light can be seen crisper than with the unaided eye.

Most of the sketches become visible if the sample is observed in a SWIR band. The pigments exhibiting transparency in NIR remain transparent in SWIR. Also, yellow/gold ochres and cadmium yellow medium become less opaque in SWIR. The sketches become barely observable under raw sienna, zinc white, and lead white. Cobalt blue and cerulean blue become darker than in NIR.

The thermographic inspection shows that the sketch is detectable under such pigments as naples yellow, naples yellow light, naples yellow red, French ultramarine, ultramarine deep, cadmium yellow, cadmium red, cerulean blue, and madder lakes, but only barely under cobalt blue and sap green.

4.2 The wooden panel with introduced delamination

The images made in visible, NIR, and SWIR bands show no presence of the defect (fig. 3). The white ground layer is barely visible under the thin layers of paint. The brushstrokes are also visible in the green background. The SWIR image demonstrates a minor dark-colored feature in the upper left corner.

The result of the thermographic inspection reveals the contours of the delamination in the center of the panel. The contours of the drawing are suppressed. The image of the defect exhibits enough contrast to estimate its geometric parameters and can be used for painting diagnostics.

4.3 The unattributed portrait of a young woman

The background of the painting appears dark to the unaided eye; this makes it hard to observe the contours of the figure in the painting (fig. 4). Several worn areas are visible as lighter regions, which is influenced by the brighter ground layer.

NIR makes the contours of the image appear sharper. The coat of the person in the portrait remains dark; no features of the coat can be detected in this region.

The cracks around the head become darker on the SWIR image, which is probably the result of the presence of dust in the cracks. It is interesting that the worn regions appear dark in SWIR while they appear

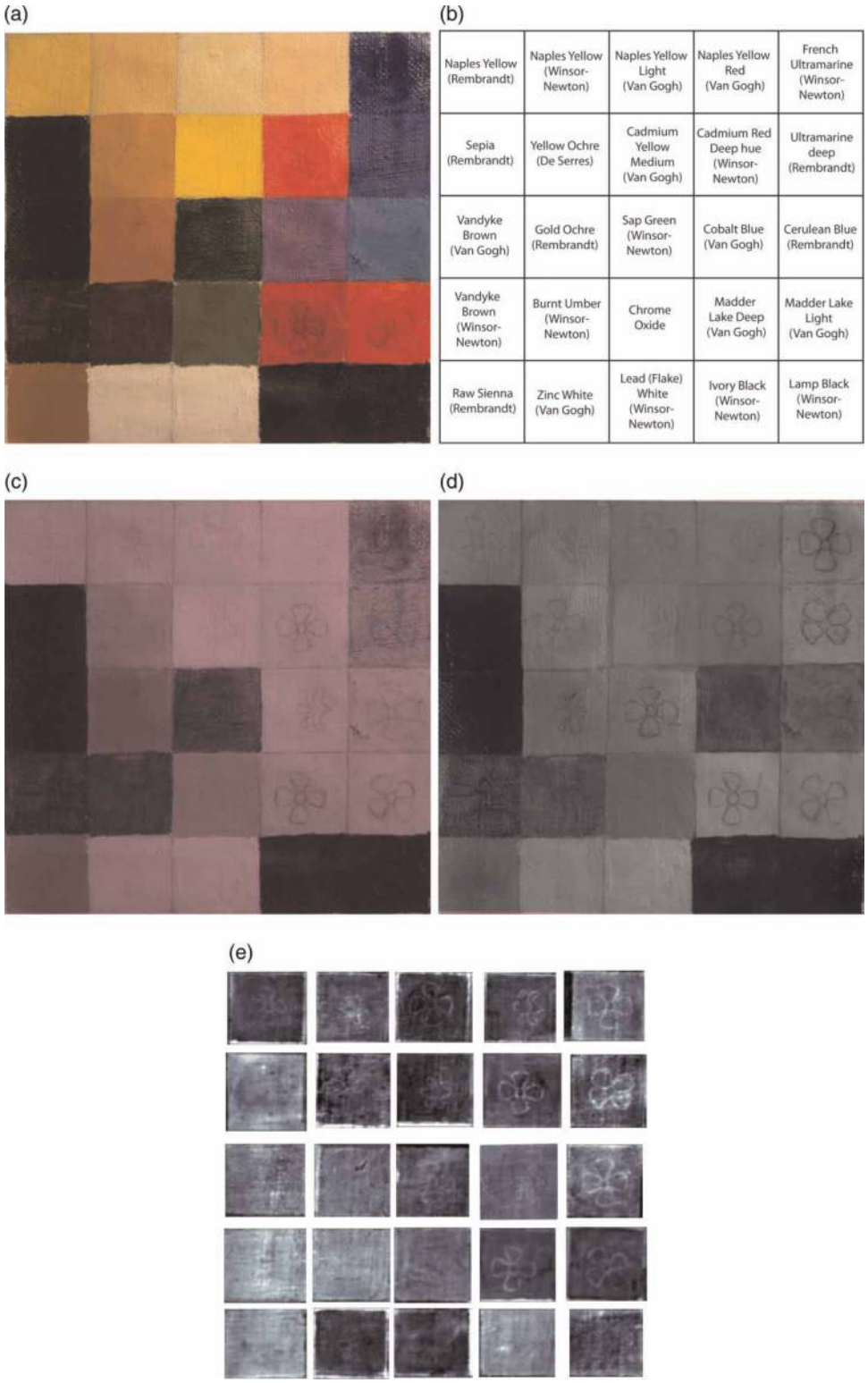

FIG. 2. The self-made canvas sample tested. Oil on canvas. (a) The general image of the canvas sample, (b) the scheme of the materials used (manufacturers of pigments are specified in brackets), (c) near-infrared image of the sample (made with a silicon CCD detector, spectral band: 0.7–1.1 μm), (d) SWIR image of the sample (made with InGaAs detector, spectral band: 0.9–1.7 μm), (e) individual thermographic images collected from the sample (MWIR spectral band, 3–5 μm, principal component processing applied).

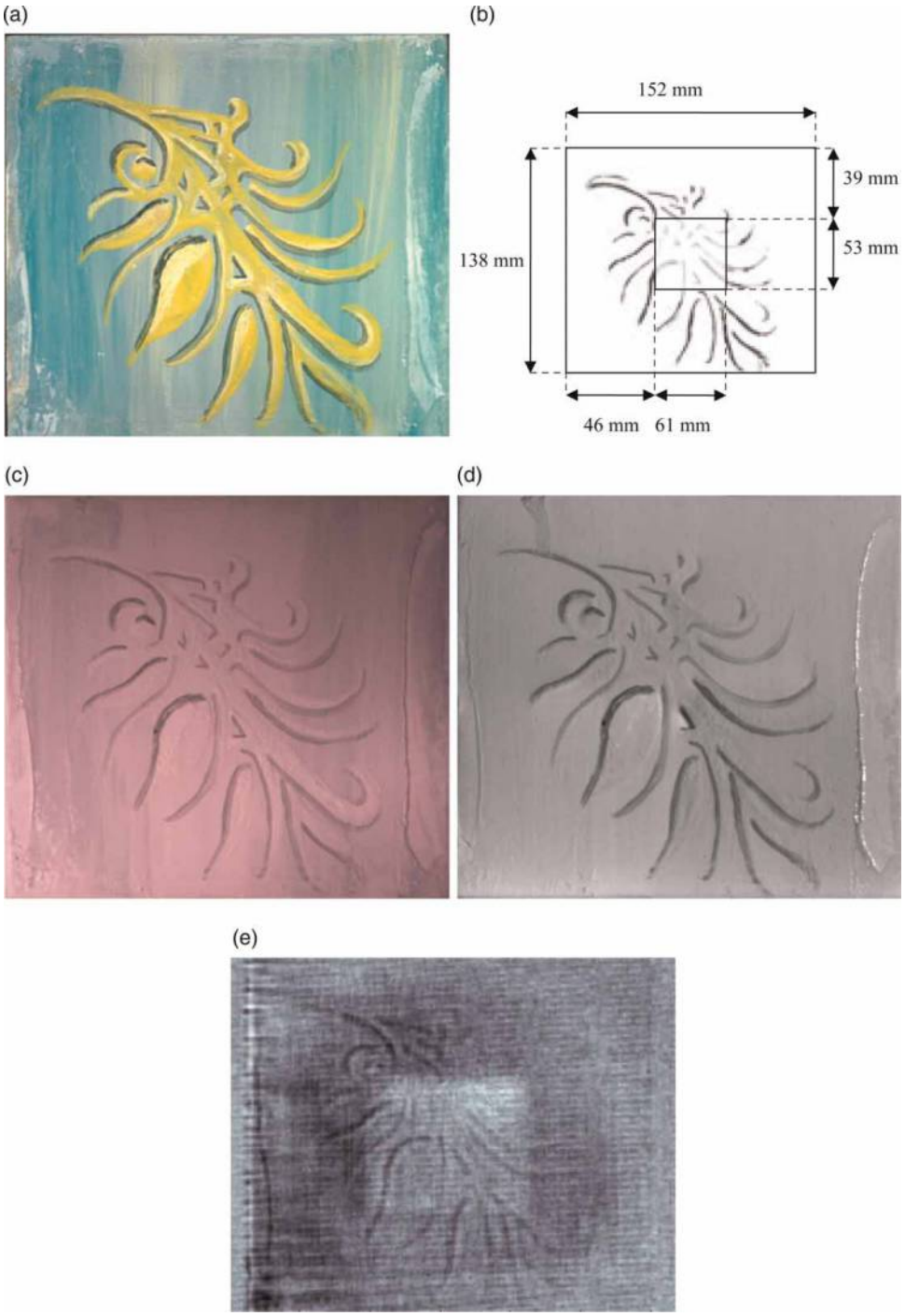

FIG. 3. The self-made sample, mimicking a panel painting. Oil, tempera, wood. (a) The general image of the sample, (b) the scheme of the defect location, (c) near-infrared image of the sample (made with a silicon CCD detector, spectral band: 0.7–1.1 μm), (d) SWIR image of the sample (made with InGaAs detector, spectral band: 0.9–1.7 μm), (e) thermographic image collected from the sample (MWIR spectral band, 3–5 μm, principal component processing applied).

bright in NIR. The coat remains impenetrable for infrared, thus making the detection of any pentimenti in this region difficult.

On the image representing the result of the thermographic inspection the thin contours of the craquelure become suppressed by the image-processing procedure. The technique allowed for distinguishing a detail of the portrait that was painted over—the necklace with a cross, which is invisible in both NIR and SWIR images.

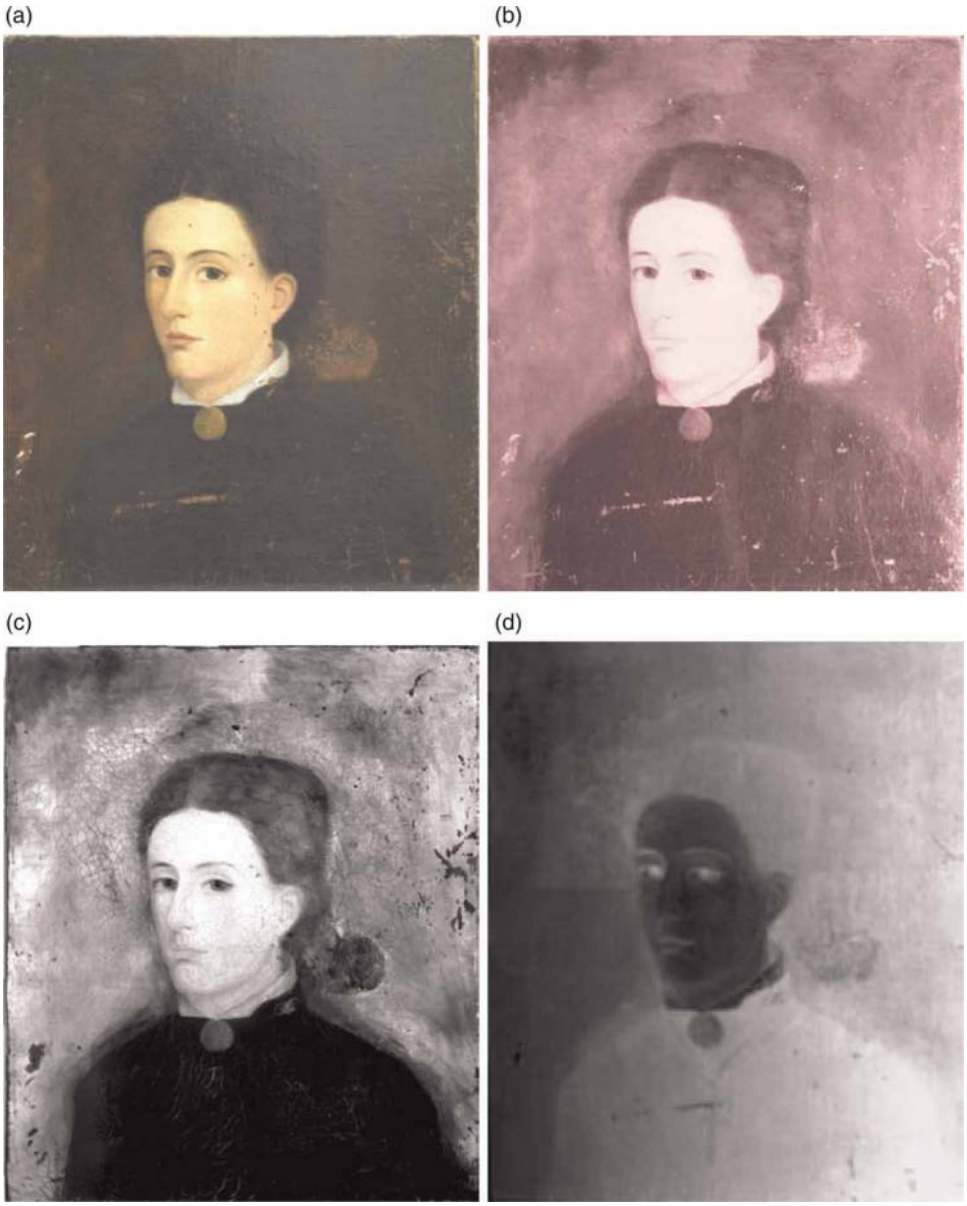

FIG. 4. The portrait tested. Unattributed. Portrait of a young woman. Oil on canvas. 49.5 cm × 41.8 cm. Owned by a private collector, Windsor, Canada. (a) The general image of the painting, (b) near-infrared image of the painting (made with a silicon CCD detector, spectral band: 0.7–1.1 μm), (c) SWIR image of the painting (made with an InGaAs detector, spectral band: 0.9–1.7 μm), (d) mosaic thermographic image collected from the portrait (MWIR spectral band, 3–5 μm, principal component processing applied).

4.4 THE PORTRAIT OF A MUSICIAN BY THOMAS FAED

On the image made in visible band, the background appears dark; no degraded or altered regions are observable (fig. 5). The image made in NIR band demonstrates brushstrokes on the background. Some of the sketches are visible including the lines on the sleeve and the musician's jacket. Presumably, the contours of the lapel were different at the stage of the sketch. SWIR image demonstrates nearly the same observations as the NIR image. However, the overall quality of the image is different. The main difference is the contrast of the sketches found, which is more visible than in NIR.

The analysis of the thermographic image shows the presence of the same sketches as those detected in NIR and SWIR: the thin lines are visible in the regions of the lapel and the sleeve, as was observed on the simulated sample with lead pencil sketches. Some restored regions can be observed in the face area.

FIG. 5. The portrait tested. Thomas Faed, Portrait of an old musician with flute. Oil on canvas. 35.8 × 25.5 cm. Owned by a private collector, Windsor, Canada. (a) The general image of the painting, (b) near-infrared image of the painting (made with a silicon CCD detector, spectral band: 0.7–1.1 μm), (c) SWIR image of the painting (made with an InGaAs detector, spectral band: 0.9–1.7 μm), (d) mosaic thermographic image collected from the painting (MWIR spectral band, 3–5 μm, principal component processing applied).

4.5 THE ICON

The painting contains certain losses of paint where the exposed ground layer is visible (fig. 6). The top part of the panel bears signs of some wear where part of the paint is rubbed off. The losses are observable in the image made in visible band.

The NIR image demonstrates the shape of the brushstrokes. The rubbed regions on the top edge exhibit

FIG. 6. The icon tested. Unattributed. Madonna with Child. Tempera on wood. 28 × 20.5 cm. Owned by a private collector, Windsor, Canada. (a) The general image of the painting, (b) near-infrared image of the painting (made with a silicon CCD detector, spectral band: 0.7–1.1 μm), (c) SWIR image of the painting (made with an InGaAs detector, spectral band: 0.9–1.7 μm), (d) mosaic thermographic image collected from the painting (MWIR spectral band, 3–5 μm, principal component processing applied).

more contrast than in the visible image. No sketches were found except for several thin lines on the Christ figure, which are also detectable in the visible image.

In the SWIR image the sketches become observable (e.g. descending lines to the left of Holy Mary's head or a primary contour for her hand in the right part of the panel). The crowns become transparent as well as the blue coats. White imprintings become almost invisible. The brushstrokes are easily observable. The rubbed regions on the top edge expose less contrast than in NIR since the background color becomes transparent and the white ground layer becomes observable underneath.

In the thermographic image, one can distinguish the grain structure of wood as well as a big delamination

in the top left corner. Most probably, the delamination is formed under the surface layers of wood, which is indicated by grain contours of wood overlaying the image of the delamination itself. Another defect can be seen in the lower left corner where the dim image of a delamination apparently is not overlaid with the grain pattern. This may indicate the presence of a delamination between the ground layer and the support.

5. Discussion

In this work three nondestructive techniques of analysis of artworks were compared. These included NIR, SWIR, and thermographic approaches of paintings inspection. The comparison was done from the point of view of their detection capabilities of artwork degradation and artifacts covered with different paints. For the purpose of comparison a set of samples was used, which included specially prepared ones as well as real artworks.

The first part of the work was devoted to the comparison of two closely related methods – the analysis of paintings in NIR and SWIR spectral bands. Although according to studies by various authors most of the artistic materials exhibit maximum transparency at wavelengths around 2 μm, they still can be looked through at shorter wavelength. The latter allows for using silicon CCD cameras, which are much less expensive than the detectors working in SWIR band.

It can be seen that ultramarine, cobalt blue, and cerulean blue exhibit high transparency in the NIR band (observed with a silicon CCD camera, 0.7–1.1 μm). The sketches can barely be seen under such pigments as naples yellow, yellow ochre, and cadmium yellow. Other pigments demonstrated poor transparency. In SWIR band (observed with InGaAs camera, 0.9–1.7 μm), naples yellow pigments become much more transparent as well as ultramarine and ochre. Sketches become barely detectable under raw sienna, burnt umber, zinc white, and lead white. It is noteworthy that cobalt blue and cerulean blue become less transparent in SWIR than in NIR (figs. 2c, 2d).

Such pigments as sepia, Van Dyke brown, chrome oxide, ivory black, and lamp black demonstrate no transparency in either of NIR and SWIR spectral bands. The main reason for this is the high concentration of carbon in these materials, which not only attenuates infrared waves, but also makes it impossible to distinguish between the carbon-containing paint material and the lines made with lead pencil, which contain carbon as well.

Due to the absence of graphite sketches on the ground layer of the simulated panel painting, the images of the sample tested look almost similar in both NIR and SWIR bands (figs. 3c, 3d). The introduced defect remained undetected with either NIR or SWIR due to the thickness of the gesso layer (the total thickness of the ground and the paint layers was approximately 0.25 mm).

The studies of real oil paintings on canvas demonstrated the increased contrast of the NIR and SWIR images compared to the image detected by the unaided eye (figs. 4, 5). On the portrait of the young woman the coat appears to be absolutely opaque to both NIR and SWIR, which is most probably the consequence of a high concentration of carbon in the black paint used for the drawing of the coat. For this reason, no sketch or alteration can be detected in this region with NIR and SWIR. In contrast to this, the coat of the musician, depicted on another painting examined, demonstrates enough transparency in NIR and SWIR for the sketches to be detectable.

The study of a tempera icon demonstrated nearly the same results, namely the increase in the overall contrast of the NIR and SWIR images with respect to the image made in visible band. The sketches corresponding to Madonna's crown and her veil are barely observable on the SWIR image.

The second part of the work was to compare the results of NIR and SWIR analysis to those collected from the thermographic method utilizing longer wavelengths (3–5 μm) for the detection of temperature fields on the surface of the sample studied after its stimulation with a flash. On the sample mimicking a canvas with graphite sketches thermographic study demonstrated the presence of the sketches under layers of naples yellow, ultramarine, cobalt blue, and cerulean blue. The sketches can barely be seen under yellow ochre and cadmium (fig. 2e). The graphite sketch is so thin that this would not affect the surface temperature when measuring it. For this reason, the detected image is most likely produced by a direct reflection of the light from the graphite layer. The paint layer does not block the flash light entirely and the light can reflect from the graphite sketch, thus allowing us to detect the sketch by its shine.

The same effect may be visible on the "Portrait of an old musician with flute," where the sketch is barely observable on the thermographic image as a number of thin dark lines. In contrast to the previous example, the sketch does not appear in the form of bright lines in this case, which is the result of principal component processing. These lines barely appear on nonprocessed thermographic images in the form of bright strokes, which demonstrates that the results of thermographic analysis may be different depending on the processing.

The capabilities of thermographic study become evident when the sample contains a subsurface feature capable of causing enough thermal contrast. In the case of the "Portrait of a young woman," the cross on

the necklace remained undetected by NIR and SWIR methods due to the high concentration of carbon in the paint. It appears that the cross itself was made with a different paint, which made it possible to detect the presence of a foreign material under the surface.

The same principle worked in the case of defect detection. A subsurface delamination blocks the heat propagation into the bulk of material, thus making the surface temperature above the defective region different from the surface temperature above nondefective areas (figs. 3e, 6d).

6. Conclusions

- Thermography proved to be more applicable for the search of subsurface defects that may remain undetected with NIR and SWIR. Taking into account the fact that thin delaminations may be invisible in X-ray analysis, thermography can be a good alternative for defectoscopy of paintings.
- Thermography can detect some graphite sketches under thin layers of paint. Most probably this is due to direct reflection of light from the graphite ("shine"). On the other hand, NIR and SWIR devices are better suited for this purpose.
- Thermography can detect details of paintings that are hidden under layers of paint and undetectable with NIR and SWIR devices.
- It is important to remember that though principal component processing allows for enhancing the overall quality of the thermographic image, it may alter the final contrast of the image in such a way that the regions which appeared bright on the raw image (warmer areas) appear dark after processing and vice versa. The image after principal component processing does not represent temperature distributions anymore and can be used for qualitative image analysis only.

Acknowledgments

This research was performed with support from the Institute for Diagnostic Imaging Research and from the Premier of Ontario Catalyst Award for the best innovation in 2007. The team would like to express their gratitude to Tessonics Corp., Canada, and the University of Windsor, Canada, for their infrastructure support.

References

Ambrosini, D., C. Daffara, R. Di Biase, D. Paoletti, L. Pezzati, R. Bellucci, and F. Bettini. 2010. Integrated reflectography and thermography for wooden paintings diagnostics. *Journal of Cultural Heritage* 11:196–204.

Avdelidis, N. P., and A. Moropoulou. 2004. Applications of infrared thermography for the investigation of historic structures. *Journal of Cultural Heritage* 5:119–27.

Avdelidis, N. P., M. Koui, C. Ibarra-Castanedo, and X. Maldague. 2007. Thermographic studies of plastered mosaics. *Infrared Physics and Technology* 49:254–56.

Bendada, A., S. Sfarra, D. Ambrosini, D. Paoletti, C. Ibarra-Castanedo, and X. P. V. Maldague. 2010. Active thermography data processing for the NDT&E of frescoes. 10th International Conference on Quantitative InfraRed Thermography. Quebec, July 27–30, 2010.

Blessley, K., C. Young, J. Nunn, J. Coddington, and S. Shepard. 2010. The feasibility of flash thermography for the examination and conservation of works of art. *Studies in Conservation* 55:107–20.

Daultrey, S. 1976. *Principal components analysis*. Norwich: Geo Abstracts Ltd.

Desneux, J. 1958. Underdrawings and pentimenti in the pictures of Jan Van Eyck. *The Art Bulletin* 40:13–21.

Falco, C. M. 2009. Invited article: High resolution digital camera for infrared reflectography. *Review of Scientific Instruments* 80:071301–07301–9.

Farnsworth, M. 1938. Infrared absorption of paint materials. *Technical Studies in the Field of the Fine Arts* 7:88–98.

Friedel, R. A., and L. J. E. Hofer. 1970. Spectral characterization of activated carbon. *The Journal of Physical Chemistry* 74:2921–2.

Friedel, R. A., and L. J. E. Hofer. 1971. Infrared spectra of ground graphite. *The Journal of Physical Chemistry* 75:1149–51.

Gargano, M., N. Ludwig, and G. Poldi. 2007. A new methodology for comparing IR reflectographic systems. *Infrared Physics and Technology* 49:249–53.

Gavrilov, D., C. Ibarra-Castanedo, E. Maeva, O. Grube, X. Maldague, and R. Gr. Maev. 2008. Infrared methods in noninvasive inspection of artwork. Proceedings of 9th Intern. Conf. on 'Non-Destructive Investigations and Microanalysis for the Diagnostics and Conservation of Cultural and Environmental Heritage. Jerusalem, Israel, 040-1-040-8.

Gavrilov, D., C. Kais, E. Maeva, and R. Gr. Maev. 2010. A comparison of near- and mid-infrared band reflectography for the aids of artwork diagnostics. Proceedings of 10th International Conference on Quantitative Infrared Thermography. Quebec, Canada, 975–80.

Grinzato, E., P. Bison, S. Marinetti, and V. Vavilov. 1994. Nondestructive evaluation of delaminations in Fresco plaster using transient infrared thermography. *Research in Nondestructive Evaluation* 5:257–74.

Grinzato, E., G. Cadelano, P. Bison, F. Peron, and X. Maldague. 2010. High resolution and automatic survey of buildings by IR thermography. 10th International Conference on Quantitative InfraRed Thermography. Quebec, July 27–30.

Heiber, W. 1968. The use of an infra-red image-converter for the examination of panel paintings. *Studies in Conservation* 13:145–9.

Hermosilla-Lara, S., P. Y. Joubert, D. Plasko, F. Lepoutre, and M. Piriou. 2002. Enhancement of open-cracks detection using a principal component analysis/wavelet technique in photothermal nondestructive testing. *Proceedings of*

6th International Conference on Quantitative Infrared Thermography. Dubrovnik, Croatia, September 24–27.
Jolliffe, I. T. 2002. *Principal components analysis*. New York: Springer.
King, E. 1936. Notes on the paintings by Giovanni Di Paolo in the Walters collection. *The Art Bulletin* 18:214–39.
Lyon, A. 1934. Infra-red radiations aid examination of paintings. *Technical Studies in the Field of the Fine Arts* 2:203–12.
Maldague, X. 2001. *Theory and practice of infrared technology for non-destructive testing*. New York: John Wiley & Sons.
Meola, C., R. Di Maio, N. Roberti, and G. M. Carlomagno. 2005. Application of infrared thermography and geophysical methods for defect detection in architectural structures. *Engineering Failure Analysis* 12:875–92.
Miller, B. 1977. The feasibility of using thermography to detect subsurface voids in painted wooden panels. *Journal of the American Institute for Conservation* 16 (2):27–35.
Moss, T. S. 1959. *Optical properties of semi-conductors*. London: Butterworths Scientific Publications.
Rajic, N. 2002. Principal component thermography for flaw contrast enhancement and flaw depth characterization in composite structures. *Composite Structures* 58:521–8.
Vavilov, V. P., D. A. Nesteruk, V. V. Shiryaev, and W. Swiderski. 2008. Application of principal component analysis in dynamic thermal testing data processing. *Russian Journal of Nondestructive Testing* 44:509–16.
Van Asperen de Boer, J. R. J. 1968. Infrared reflectography: A method for the examination of paintings. *Applied Optics* 7:1711–4.
Van Asperen de Boer, J. R. J. 1969. Reflectography of paintings using an infrared vidicon television system. *Studies in Conservation* 14:96–118.
Wright, D. A. 1966. *Semi-conductors*. London: Methuen & Co. Ltd.

Equipment And Suppliers

FLIR SC4000
FLIR Systems Ltd.
5230 South Service Road Suite 125
Burlington, Ontario, Canada, L7L 5K2
www.flir.com/thermography/americas/us/
(866) 477-3687

XenICs Xeva 1.7-320 camera
XenICs Infrared Solutions
Ambachtenlaan 44 BE-3001
Leuven, Belgium
www.xenics.com

Fujifilm Finepix S3 Pro UVIR camera
Fujifilm Canada Inc.
600 Suffolk Court
Mississauga, Ontario, Canada, L5R 4G4
www.fujifilm.ca

Speedotron 4803CX system and 206VF light unit
Speedotron
310 South Racine Avenue
Chicago, IL, USA, 60607-2841
www.speedotron.com

Wratten 87 – Infrared-pass filter
PECA Products Inc.
471 Burton Street
Beloit, WI, USA, 53511
www.pecaproducts.com
Phone (800) 999-7322
Fax (608) 299-1827

Author Biographies

Dmitry Gavrilov graduated from Moscow Engineering Physics Institute in 2005, and now is a PhD student and researcher at the Institute for Diagnostic Imaging Research (IDIR), Windsor, Canada. His field of work includes noninvasive methods of analysis of multilayered structures—preliminary diagnostics and authentication of objects of art, such as canvas- and wood-based paintings. The spectrum of interests includes infrared and ultraviolet radiographies, X-ray and advanced thermographic methods of analysis as well as art materials characterization with the aid of X-ray fluorescence, Raman spectroscopy, and mass spectrometry. Address: Department of Physics, 401 Sunset Ave., University of Windsor, Windsor, ON, Canada N9B 3P4. Email: gavrilo@uwindsor.ca

Dr. Elena Maeva is an associate professor in the Department of Physics, University of Windsor, Ontario, Canada. She received combined BSc and MSc degrees from D. Mendeleev's University of Chemical Technology of Russia, with specialization in physics and chemistry of polymers. She obtained her PhD degree in material science with specialization in physics and chemistry of polymers from the Institute of Physical Chemistry of Russian Academy of Sciences. Her research areas are the nondestructive methods of investigation of physical, mechanical, and chemical properties of composite, biocomposite materials, the environmental effects on the materials properties, and degradation processes. She is the Chair of the Division of Industrial and Applied Physics (DIAP) of Canadian Association of Physicists (CAP). Address: as for Gavrilov. Email: maeva@uwindsor.ca

Oleg Grube graduated from Latvian Academy of Arts in 1974. At the same time he started to study and work as a restorer of oil paintings in the Museum of Latvian and Russian Classical Art in Riga, Latvia. Oleg Grube worked in various museums in Riga. Before coming to Canada in 1997 he was the Head of Conservation Department in the Museum of the History of Medicine of

Latvia. He practiced restoration and gave his expert opinion in Canada, Germany, and Denmark. To date, he has been employed as the pictorial art expert in "Gallery Sixty-eight Auctions" auction house. Address: Tessonics Inc., 1983 Ambassador Dr., Windsor, ON, Canada N9C 3R5.

Dr. IGOR VODYANOY is a Program Manager at the Office of Naval Research (ONR). He is also a visiting professor at the Imperial College London, where he is carrying out an advanced research program in membrane biophysics using Conducting Ion Microscopy. He also served as Science Adviser to Warfighter Performance Department Head and Associate Director of ONR Europe for science and technology. Dr. Vodyanoy received his education at Leningrad Polytechnic Institute and Institute of Cytology USSR Academy of Sciences. He pursued academic research in biophysics at the University of California Irvine, at NIH and since 1988 at ONR. He has authored about 80 research papers, edited books and organized a number of scientific meetings. His research revealed fundamental properties of polymer transport and water properties in nano-sized water pores. His current research interest is in biological signal transduction, stochastic resonance phenomenon, and cell membrane dynamics. Dr. Vodyanoy is also interested in art examination technologies. Address: Office of Naval Research, 875 N. Randolph St., Suite 1425, Arlington, VA 22203-1995, USA. Email: igor.vodyanoy@navy.mil

Dr. ROMAN GR. MAEV received combined BS and MSc degrees from the Moscow Engineering Physics Institute in 1969, and PhD from the Physical N. Lebedev Institute of the Russian Academy of Sciences in 1973. In 2001, he received a Dr Sc and in 2005 Full Professor Diploma in Physics from the Russian Federation Government. In 2008, Dr. Maev was appointed Director General of the Institute of Diagnostic Imaging Research, Windsor, Ontario, Canada. He has published over 300 articles, various reviews, three monographs, and holds 23 patents. Dr. Maev holds many awards for his research results, most notably: Centenary Ernst Abbe Medal, 1989; Ontario Premier's Catalyst Award and Canadian Association of Physicists Gold Medal, both in 2007. Address: Institute for Diagnostic Imaging Research, 401 Sunset Ave., University of Windsor, Windsor, ON, Canada N9B 3P4. Email: maev@uwindsor.ca

Résumé–Cet article décrit les méthodes non destructives d'imagerie pour l'examen des peintures telles que le proche infrarouge, l'infrarouge à ondes courtes et la thermographie, tout en les comparant dans leur habileté à révéler des dessins sous-jacents au graphite et des dégradations cachées sous la surface picturale. Ces méthodes d'examen permettent de mieux comprendre la technique picturale de l'artiste et de localiser des zones de dommage invisibles à la surface. Alors que les trois méthodes sont adéquates pour localiser des ébauches et des changements dans la composition, cette étude a prouvé que les méthodes thermographiques sont très utiles dans la détection de défauts dans la structure des couches, tels que les décollements et les cavités, comme l'ont démontré les essais menés sur des éprouvettes et de vraies peintures.

Resumen–Métodos no invasivos de infrarrojo cercano, infrarrojo de onda corta e inspección termografía de obras de arte son descritos en este articulo y comparados en termino de su habilidad para revelar tanto los dibujos de grafito escondidos debajo de la pintura, como la degradación por debajo de la superficie. Esta inspección contribuye a entender los métodos de trabajo de los artistas y ubica áreas ocultas de daño. Siendo que los tres métodos de inspección son apropiados para ubicar bosquejos y cambios en la composición, este estudio comprobó que los métodos termográficos son muy útiles para detectar defectos estructurales tales como delaminación y cavidades, como se pudo demostrar por medio de experimentos hechos en muestras de prueba y en pinturas reales.

Resumo–Métodos não-invasivos de infravermelho próximo, infravermelho de ondas curtas e inspeção termográfica de obras de arte são descritos neste artigo e comparados em termos de sua capacidade de revelar tanto a grafite oculta sob os desenhos quanto as degradações da subsuperfície. Esta inspecção auxilia a compreensão dos métodos de trabalho do artista e localiza áreas de danos ocultas. Embora todos os três métodos de inspeção sejam adequados para determinar a situação de esboços e alterações da composição, este estudo demonstrou que os métodos termográficos são muito úteis para a detecção de defeitos estruturais, tais como delaminações e cavidades, como foi demonstrado pelos experimentos realizados com amostras de teste e pinturas reais.